PAPER • OPEN ACCESS

TIG and MIG welding of high strength Cr-Mn and Cr-Ni alloyed austenitic stainless steel combinations

To cite this article: E Kalácska *et al* 2018 *IOP Conf. Ser.: Mater. Sci. Eng.* **426** 012021

IOP Conf. Series: Materials Science and Engineering **426** (2018) 012021 doi:10.1088/1757-899X/426/1/012021

TIG and MIG welding of high strength Cr-Mn and Cr-Ni alloyed austenitic stainless steel combinations

E Kalácska[1], B Varbai[1], J Ginsztler[1] and K Májlinger[1]

[1] Budapest University of Technology and Economics, Department of Materials Science and Engineering, Budapest, Hungary

E-mail: welding@att.bme.hu

Abstract. To substitute the relative expensive Ni alloying in stainless steels manganese alloying can be used. The welding of Cr-Mn alloyed steels however is not very well documented. In our current research two Cr-Mn alloyed austenitic stainless steel grades (1.4371 and 1.4376) were welded together via tungsten inert gas welding (TIG) and metal inert gas welding (MIG). Also for comparison different joint combinations with other Cr-Ni alloyed steel grades (1.4318 and 1.4301) were welded. The different steel grade showed quite the different behaviour in the joint combinations. The Mn-content in the base materials increased the weld metal hardness and tensile strength of the joint and decreased the fracture elongation values. Also the Mn-alloyed grades had significant higher grain coarsening in the heat affected zones than the Cr-Ni alloyed.

1. Introduction

As the influence of automotive, oil and gas, and chemical industries is constantly growing, high strength steels, aluminum alloys and corrosion resistant steels gain more attention [1–9]. In these industries austenitic stainless steels (ASSs) are the most widely used corrosion resistant grades [10, 11].

The conventional ASSs, such as 1.4301 and 1.4404 have a relatively high nickel alloying content (Ni = 8–10 wt.%) next to chromium (Cr ~ 18 wt.%). However, recently in order to substitute the relatively expensive Ni in ASS grades manganese (Mn) and nitrogen (N) alloying is used [11, 12]. The austenite forming effect of high Mn (up to 9 wt.%) and N content (up to 0.3 wt.%) also comes together with higher mechanical strength [13–15]. Comparing to the conventional austenitic stainless steels, which has yield strength ($R_{p0.2}$) is around 200 MPa, the Mn and N alloyed grades reach above 600 MPa $R_{p0.2}$. Despite of the lower base material price and higher strength of Cr-Mn alloyed ASSs, the corrosion resistance is usually lower [16–19] and their weldability is not well documented in the literature.

The mechanical properties of low Ni ASSs after welding is found to be sensitive to the grain size and structure [20–22]. Lower heat input resulted smaller dendrite sizes and higher mechanical strength. The mechanical strength of welded low Ni ASS grades also depends on the used filler material. Researchers [23] found that using conventional filler wires (e.g. ER 308 LSi) resulted no decrease of mechanical strength of the welded joint. With the growing application of low Ni austenitic grades, their dissimilar joints to conventional high strength or corrosion resistant steels also gaining interest [24–26]. Generally, the dissimilar welding of conventional austenitic and low Ni, high N grades can be successfully made [27], this area still has a lot of research interest.

2. Materials and methods

In our current research the two used Cr-Mn alloyed ASS's were 1.4371 and 1.4376, both are additionally alloyed with nitrogen to increase yield and tensile strength and corrosion resistance. For comparison the Cr-Ni alloyed 1.4318 grade (with additional N alloying) and the most common 1.4301 normal strength austenitic steel grade were used. For both TIG and MIG welding tests the same grade (1.4316) austenitic filler was used. The microstructure of the sheets can be seen in Figure 1. All grades were fully austenitic, the high strength grade with relatively small grain size (Table 1). The chemical compositions, Cr- and Ni-equivalent and mechanical properties of the used steel grades are also listed in Table 1

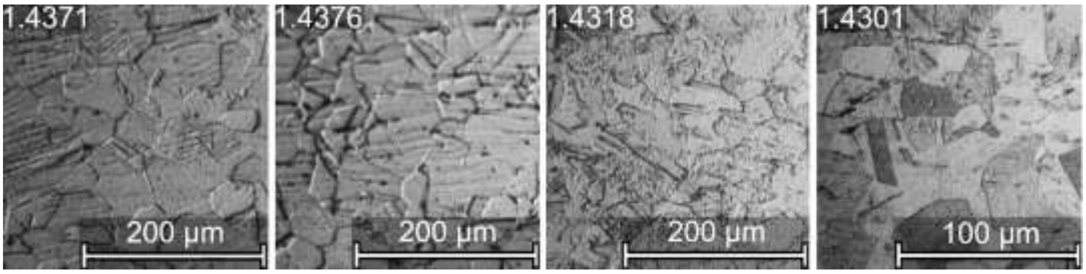

Figure 1. Microstructure of the used ASS sheets

Table 1. Main properties of the used ASS sheets and filler metal

Steel grade	Chemical composition (wt%)											Mechanical properties				Grain size (µm)
	C	Cr	Ni	Mn	Si	Mo	Cu	N	Fe	Cr_{eq}*	Ni_{eq}*	$R_{p0.2}$** (MPa)	R_m** (MPa)	A** (%)	Hardness (HV0.5)	
1.4371	0.05	15.8	4.4	7.7	0.5	0.1	0.4	0.2	bal.	16,7	15,8	620	760	25	277±10	12
1.4376	0.11	17.1	3.8	7.2	0.6	-	0.5	0.2	bal.	18,0	16,8	405	740	40	251±10	11
1.4318	0.05	16.5	7.3	1.6	0.5	0.2	0.3	0.2	bal.	17,5	15,6	350	660	35	205±2	10
1.4301	0.05	18.3	8.6	1.8	0.4	0.2	0.4	-	bal.	19,1	11,0	190	620	35	187±5	22
1.4316^W	0.02	19.9	9.1	1.8	0.9	0,1	0,3	-	bal.	21.3	10,6	390	590	35	195±4	-
1.4316^R	0,02	19.8	9.8	1.9	0.6	0,1	0,1	-	bal.	20.9	11.3	390	590	35	195±5	-

^{W} wire, ^{R} rod, *according to DeLong, ** nominal values

For the welding tests the sheets were butt welded without chamfering with ~ 1 mm gap. The sheet thicknesses were approx. 2 mm and were mechanically clamped during welding.

For the MIG welding tests ESAB LUD 450 machine was used with direct current electrode positive polarity (DC+). For shielding gas 4.6 Ar (99.996 % Ar) was used on the face and the root side with the flow rates 10 and 8 $l \cdot min^{-1}$ respectively. As filler 1.4316 grade Ø 1.2 mm wire was used.

For the TIG welding tests ESAB Aristotig 250 machine was used with direct current electrode negative polarity. For shielding gas 4.6 Ar was used on the face and the root side with the flow rates 10 and 8 $l \cdot min^{-1}$, respectively. As filler 1.4316 grade Ø 2.4 mm filler rod was used.

The measured current (I), voltage (U), welding speed (v) and the calculated heat input values (Q) for the different joint combinations for both welding processes are listed in Table 2. For the calculation of the heat input values thermal efficiency factors according to EN 1011-1:2009 standard k = 0.8 and k = 0.6 were used for MIG and TIG welding, respectively.

From the welded sheets cross sectional metallography and tensile specimens were cutout, perpendicularly to the weld seam.

The quasistatic tensile tests (according to EN ISO 6892-1 standard) were done by MTS 810 universal materials testing machine on proportional ($l_0 = 10 \times d_0$) flat specimens (excess weld bead was grinded down), where the weld centerline was located in the middle of the tensile specimen. From each joint combinations three tensile tests were done. Tensile strength of the joints (R_m), and necking at fracture (Z) were determined. The fracture elongation of the whole specimen ($A_{11.3}$), the fracture elongation of the two sheet sides of the joints ($A_{5.65}$) and the uniform elongations (ε) of the sheet materials were also determined.

The standard metallography specimens were etched with Kalling reagent (2 g $CuCl_2$ + 40 ml HCl + 40 ml C_2H_6O) for 20 s. The images were taken by Olympus PM3 microscope. The grain sizes of the different heat affected zones; HAZ 1 at the weld pool and HAZ 2 further away near to the base material were also determined.

On the metallography specimen micro-Vickers hardness measurements (HV0.5) with Buehler 1011 type microhardness tester were done and the average hardness of the base materials and different joint parts; HAZ 1, HAZ 2 and the weld metal (WM) were measured.

Table 2. Parameters and heat input values for the MIG and TIG welding of the different joint combinations

Joints		MIG welding				TIG welding			
1. Steel grade	2. Steel grade	I (A)	U (V)	v ($cm \cdot min^{-1}$)	Q ($kJ \cdot mm^{-1}$)	I (A)	U (V)	v ($cm \cdot min^{-1}$)	Q ($kJ \cdot mm^{-1}$)
1.4371	**1.4371**	78	19.3	26.7	0.27	75	11.7	10.7	0.30
1.4371	**1.4376**	82	19.3	23.5	0.32	75	11.5	11.6	0.27
1.4371	**1.4318**	75	19.5	23.7	0.30	75	11.5	8.0	0.39
1.4371	**1.4301**	74	19.4	23.8	0.29	75	11.7	8.4	0.38
1.4376	**1.4376**	73	19.3	22.3	0.30	75	11.3	10.5	0.29
1.4376	**1.4318**	76	19.4	23.4	0.30	75	11.5	10.0	0.31
1.4376	**1.4301**	77	19.3	24.3	0.29	75	11.5	9.3	0.33

3. Results and discussion

The visual inspection of the weld beads and the cross sectional metallography showed macroscopically defect free joints for all steel combinations of MIG and TIG welding as well. Therefore these joints were further investigated.

3.1. Microstructural properties

The microstructural examinations (e.g. Figure 2, 3.) showed also no weld defects of any kind. The WM had relative large dendritic grains. To investigate the grain size evolution after welding a normalized (to the initial grain size of the base metals shown in Table 1) grain size of the HAZs is shown in Figure 4.

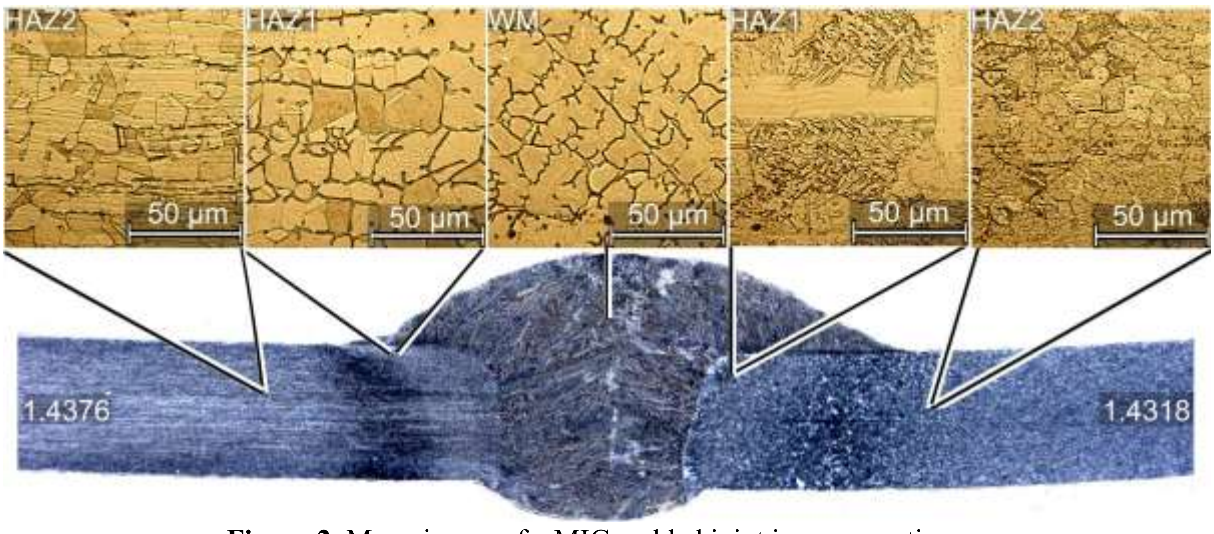

Figure 2. Macroimage of a MIG welded joint in cross section and microstructure images of the different joint zones

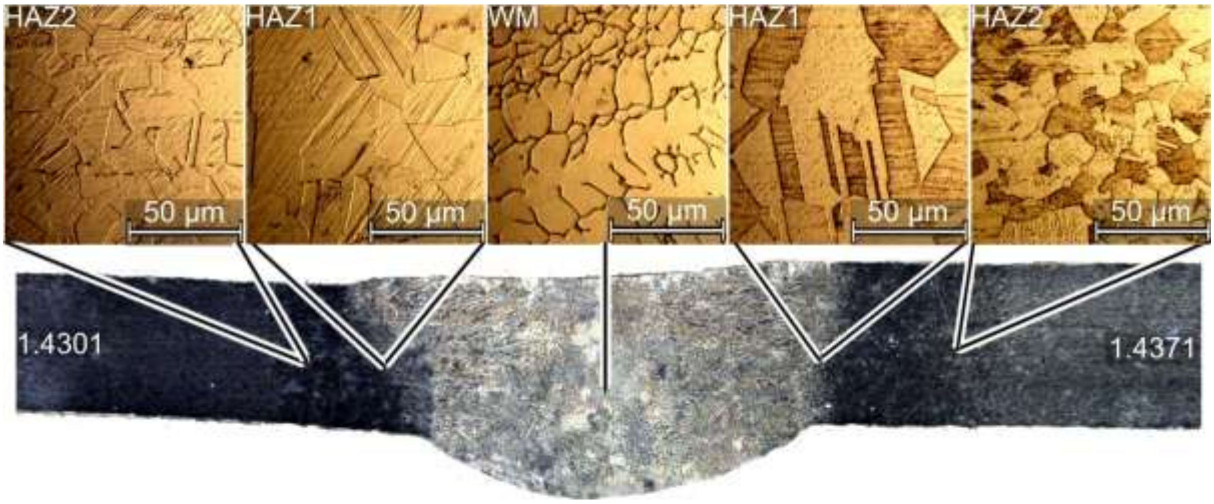

Figure 3. Macroimage of a TIG welded joint in cross section and microstructure images of the different joint zones

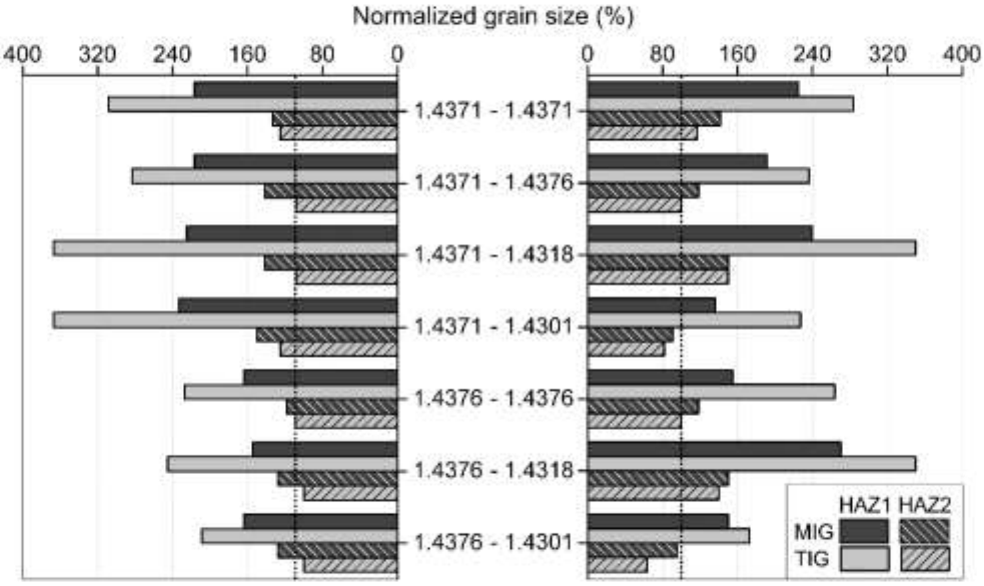

Figure 4. Normalized grain sizes in the different HAZs of the MIG and TIG welded joint combinations (vertically dotted lines corresponds to 100%)

In case of MIG welding the following trends can be observed. The highest grain coarsening occurred in the 1.4318 steel grade followed by the two Cr-Mn alloyed ones (1.4371 and 1.4376) and the normal strength 1.4301 had even smaller grains in the HAZs as the initial grain size. This trend was observed in HAZ 1 and HAZ 2 as well.

In case of the TIG welded specimens the grain coarsening order in HAZ 1 and HAZ 2 was the same with the same trends as in case of MIG welded ones (1.4318 > 1.4371 > 1.4376 > 1.4301). The absolute values were also greater than in case of MIG welding due to a "slightly" higher heat input which is also suggesting that the standardized thermal efficiency factor k = 0.6 for the TIG welding seems to be too low. Also the increment of grain sizes due to higher heat input seem to be the highest in case of the two Cr-Mn alloyed steel grades.

3.2. Hardness of the different joint parts

To investigate the effect of dilution on the weld metal hardness the normalized WM hardness (to the nominal hardness of the WM shown in Table 1) was measured (Figure 5).

In case of MIG welding all specimen showed slightly decreased hardness of the weld metal, only the 1.4371-1.4371 joint had higher hardness. However the variation between the normalized WM hardnesses were between 93–102% clear trends can be observed between the base materials Mn-content and the WM hardness. The higher the Mn-content of the two base materials the higher values of the of the WM hardness were measured. The joint with the normal strength (1.4301) steels had the lowest hardness values.

The same trends can be observed in case of the TIG welded joints, in some cases the hardness values were even higher than the MIG welded specimens.

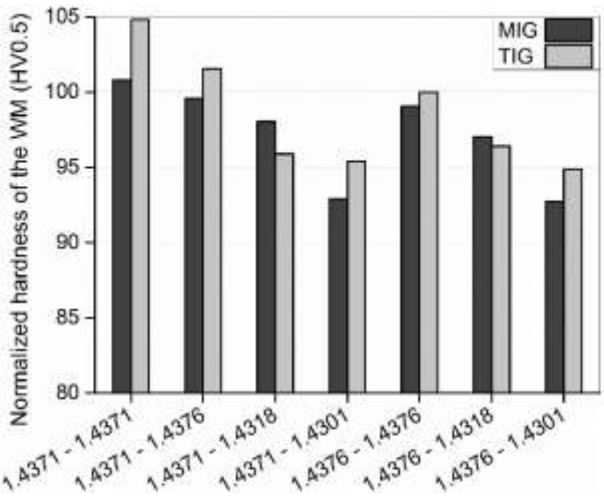

Figure 5. Normalized hardness values in the different HAZs of the MIG and TIG welded joint combinations

The increase in the WM hardness is likely the effect of Mn dilution in the WM thus Mn increases the austenite phase hardness through substitutional solid solution.

To investigate the effect of heat input in the HAZs hardness the normalized hardness values of the different joint combinations are shown in Figure 6.

In HAZ 1 (adjacent to the solidified WM) also clear trends can be observed with the Mn-content of the different steel grades for both welding methods. The greatest softening was in the 1.4371 steel grade with the highest Mn-content (1.4376) followed by the other Cr-Mn alloyed grade, than the normal strength Cr-Ni alloyed 1.4301 steel and the 1.4318 one.

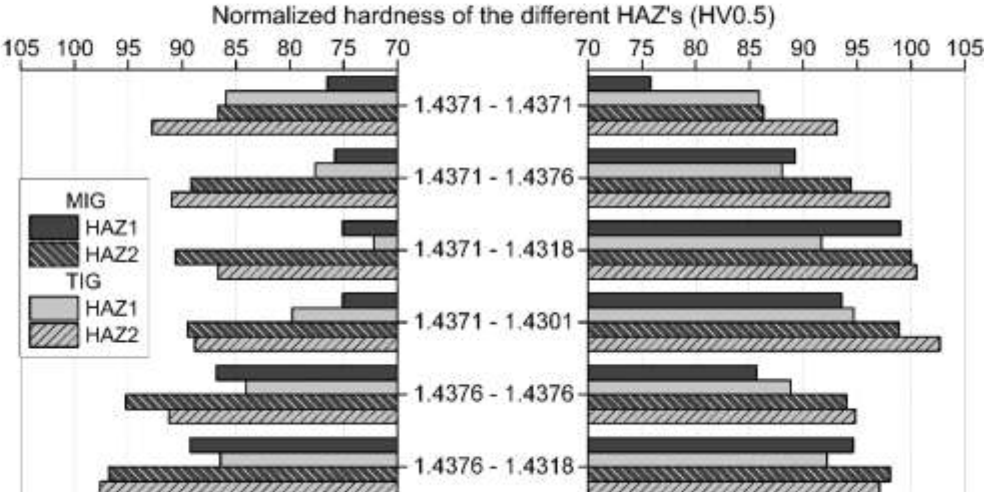

Figure 6. Normalized hardness values of the MIG and TIG welded joint combinations

In HAZ 2 also the 1.4376 steel had the greatest softening followed by the 1.4371 and the Cr-Ni alloyed had about the same hardness near to the initial base material hardness.

The large softening in the HAZ 1 cannot be attributed alone to the grain coarsening because the 1.4318 steel had the greatest grain coarsening and yet the smallest hardness decrease.

IOP Conf. Series: Materials Science and Engineering **426** (2018) 012021 doi:10.1088/1757-899X/426/1/012021

3.3. Tensile properties

In all tensile specimens the necking occurred in the WM, where the fracture of the joints also occurred. Therefore the differences in the tensile strength of the specimen can be attributed to the dilution of the base metal sheets and the filler material. The mean values of the tensile strength of the different joint combinations are illustrated in Figure 7.

In case of MIG welding the R_m values varied relatively small (between 645–675 MPa), nevertheless analogue to the WM hardness (Figure 5.) the same correlation was found. The Mn-content of the base materials increased the R_m values.

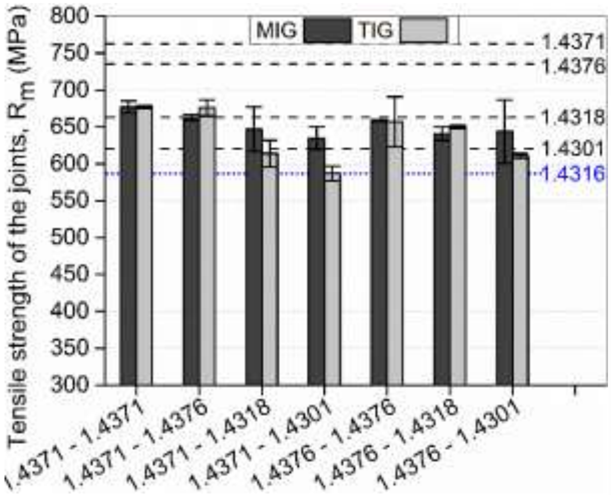

Figure 7. Tensile strength (R_m) of the MIG and TIG welded joint combinations

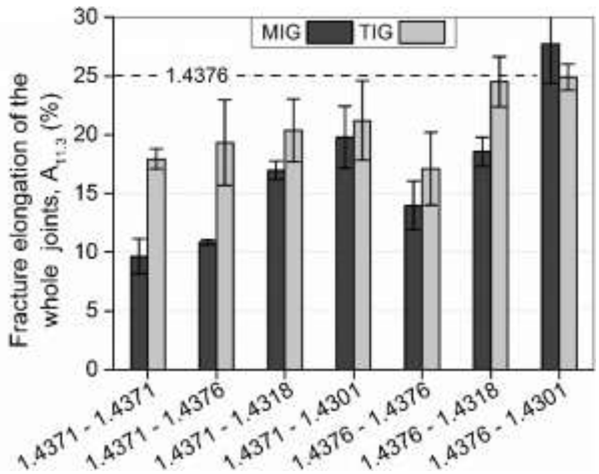

Figure 8. Fracture elongation ($A_{11.3}$) MIG and TIG welded joint combinations

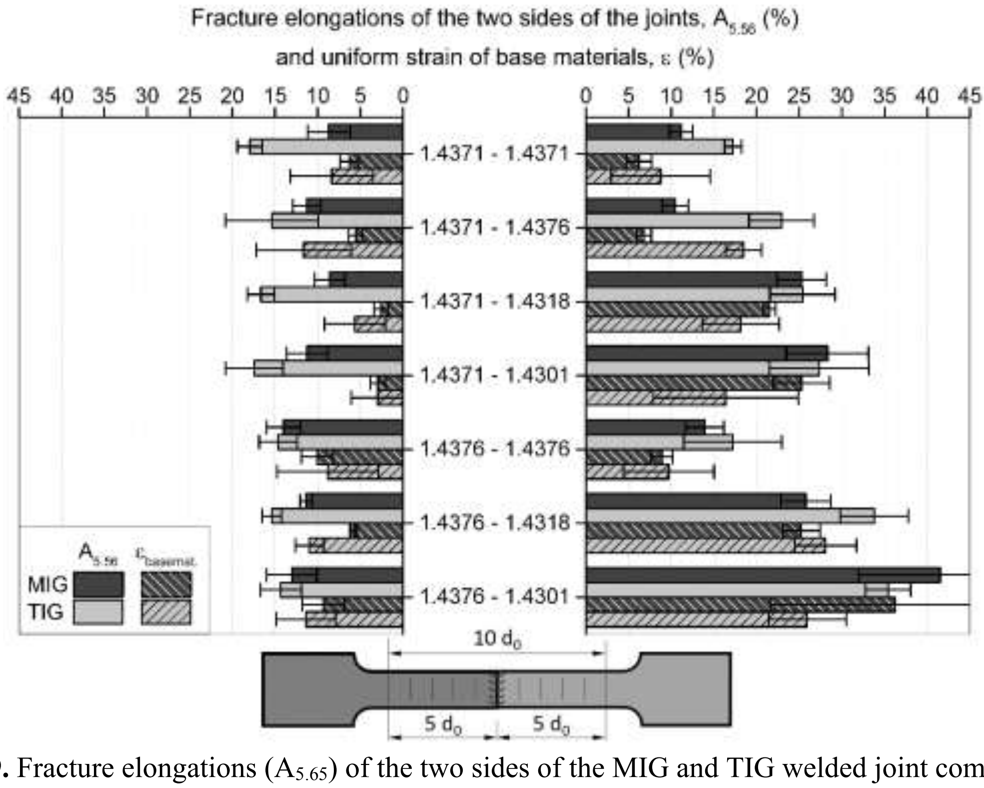

Figure 9. Fracture elongations ($A_{5.65}$) of the two sides of the MIG and TIG welded joint combinations and the uniform elongations (ε) of the base materials in these joints

In case of the TIG welded joints, R_m values varied more (575–675 MPa), and the same trends can be observed as in MIG welding.

The increase of the R_m values is also a result of the effect of Mn dilution in the WM, because Mn increases the austenite phases strength through substitutional solid solution.

To investigate the tensile response of the joined steel combinations, the fracture elongation of the whole specimen was determined (Figure 8). The $A_{11.3}$ values showed significant decrease with the increase of the Mn-content in the base materials in the joint combinations for both MIG and TIG welding.

Because all joints have at least two different base material parts (the dissimilar joint combinations three) it is interesting to see the deformations in these parts separately (Figure 9).

Du Toit and Steyn found [28] that the 1.4301 grade ASS has greater strain hardening exponent than the Cr-Mn alloyed 1.4373 grade. In case of MIG welding, we found the least deformation ($A_{5.65}$ and ε) occurred were the two Cr-Mn alloyed grades 1.4376 ≤ 1.4371 followed by the high strength Cr-Ni alloyed grade (1.4318) and the normal strength 1.4301 ASS grade. It is interesting, because the greatest hardness decrease was found in the HAZs of the Cr-Mn alloyed grades, and the grain coarsening was also high at these ASSs. These facts indicate that the strain hardening exponent of the Cr-Mn-N alloyed grades must be higher than the other used steel grades.

The necking values at fracture, and sides of the fracture within the WM are listed in Table 3. The necking values showed relative large scatter and no trends could observed, but the fracture side of the tensile specimen clearly showed the tendency that the favored fracture side was on the base material side with higher Mn-content.

Table 3. Necking at fracture, and sides of the fracture of the tensile specimens of the MIG and TIG welded joints

1. Steel grade	Fracture side						2. Steel grade	Necking at fracture Z (%)	
	MIG			TIG				MIG	TIG
1.4371	◄	◄	◄	◄	◄	●	**1.4371**	45±4	43±1
1.4371	◄	◄	◄	◄	◄	►	**1.4376**	45±1	48±9
1.4371	◄	◄	◄	◄	◄	►	**1.4318**	44±3	51±5
1.4371	◄	◄	◄	◄	►	►	**1.4301**	48±1	49±1
1.4376	◄	◄	●	◄	►	►	**1.4376**	39±4	56±6
1.4376	◄	◄	◄	►	►	►	**1.4318**	45±2	47±2
1.4376	◄	►	►	►	►	►	**1.4301**	46±5	45±4

Place of the fracture within the WM: ◄ 1st steel grade,
● WM center line, ► 2nd steel grade side

4. Conclusions

According to our investigations the following conclusions can be drawn:

- The Cr-Mn-N alloyed 1.4371 and 1.4376 high strength austenitic stainless steel grades can be welded together with good joint quality also in combination with Cr-Ni alloyed high strength 1.4318 and normal strength 1.4301 austenitic steel austenitic stainless steel grades.
- Using 1.4316 filler material with MIG process (between 0.27–0.32 $kJ \cdot mm^{-1}$ heat input range) and with TIG welding (between 0.27–0.38 $kJ \cdot mm^{-1}$ heat input range) macroscopically and microscopically defect free joints can be welded.
- In the different steel grades the order of grain coarsening for both MIG and TIG welding in both HAZs were: 1.4318 > 1.4371 > 1.4376 > 1.4301.
- The weld metal hardness increased with the Mn-content of the base materials through dilution.
- The tensile fracture occurred in every case within the weld metal, the yield strength of the joints increased with the Mn-content of the base materials through dilution.

- In HAZ 1 the hardness of the base materials decreased, the normalized hardness values and decreased with higher Mn-content of the base material and the smallest decrease was in the 1.4318 steel grade observed.
- The fracture elongations of the welded specimens were the smallest with the joints of the highest Mn-content in the base material.
- The fracture elongations measured on the two sides of the joint combinations were also the smallest by the two Cr-Mn alloyed grades 1.4376 ≤ 1.4371 followed by the high strength Cr-Ni alloyed grade (1.4318) and the normal strength 1.4301 ASS grade.
- The uniform elongation of the base materials measured on the two sides of the joint combinations showed also the same order: 1.4376 ≤ 1.4371 < 1.4318 < 1.4301.

With our research the mechanical properties of dissimilar joints, made of these austenitic stainless steel grades can be predicted.

Acknowledgements
This research was supported by Aperam and Outokumpu Distribution Hungary Kft. with the steel materials. This paper has been supported by the János Bolyai Research Scholarship of the Hungarian Academy of Sciences grant number: BO/00196/16/6 and by the National Research, Development and Innovation Office - NKFIH, OTKA PD 120865 (K. Májlinger).

References
[1] Russo Spena P et al 2016 *Steel Res. Int.* **87** 1592–600
[2] Russo Spena P et al 2015 S*teel Res. Int.* **86** 1480–9
[3] Gáspár M and Balogh A 2013 *Design, Fabrication and Economy of Metal Structures* (Berlin, Heidelberg: Springer Berlin Heidelberg) pp 463–8
[4] Lukács J and Gáspár M 2014 *Adv. Mater. Res.* **891**–**892** 563–8
[5] Lukács J 2010 *Procedia Eng.* **2** 1201–10
[6] Balogh A et al 2012 *Production Processes and Systems* **5** 79–90
[7] Boillot P and Peultier J 2014 *Procedia Eng.* **83** 309–21
[8] Haraszti F and Kovács T 2017 *IOP Conf. Series: Materials Science and Engineering* **175** 1–4
[9] Oyedemi K et al 2017 *Period. Polytech. Mech. Eng.* **61** 296
[10] Pauze N et al 2010 *Duplex World 2010 Conference* (Beaune, France)
[11] Charles J et al 2009 *Rev. Métallurgie* **106** 90–8
[12] Charles J 2007 *Rev. Métallurgie* **104** 308–17
[13] Kalácska E et al 2017 *YPIC 2017: 3rd Young Welding Professionals International Conference. 120 p.* pp 20–6
[14] Speidel M O 2006 *Materwiss. Werksttech.* **37** 875–80
[15] Pistorius P C and Toit M 2010 *The Twelth International Ferroalloys Congress; Sustainable Future* pp 911–8
[16] Khobragade N N et al 2014 *Trans. Indian Inst. Met.* **67** 263–73
[17] Shi F et al 2016 *Corros. Sci.* **107** 49–59
[18] Ha H Y et al 2016 *Mater. Charact.* **119** 200–8
[19] Sudhakaran R et al 2014 *Procedia Eng.* **97** 790–9
[20] Urade V P and Ambade S P 2016 *J. Mater. Sci. Eng.* **5** 1–6
[21] Vashishtha H et al 2014 *ISIJ Int.* **54** 1361–7
[22] Chuaiphan W and Srijaroenpramong L 2014 *J. Mater. Process. Technol.* **214** 402–8
[23] Vashishtha H et al 2016 *Sci. Technol. Weld. Join.* **21** 331–7
[24] Kalácska E et al 2017 *Mater. Sci. Forum* **885** 80–5
[25] Broggiato G B et al 2015 *Procedia Eng.* **109** 356–63
[26] Chandra-Ambhorn S et al 2012 *Adv. Mater. Res.* **538**–**541** 1464–8
[27] Vashishtha H et al 2017 *J. Manuf. Process.* **25** 49–59
[28] Du Toit M and Steyn HG 2012 *J. of Mat. Eng & Perf.* **21(7)** 1491-5